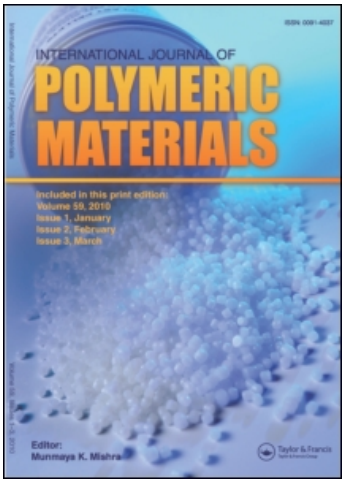

International Journal of Polymeric Materials
Publication details, including instructions for authors and subscription information:
http://www.informaworld.com/smpp/title~content=t713647664

Preparation of BPA Epoxy Resin/POSS Nanocomposites and Nonisothermal Co-curing Kinetics with MeTHPA

Jungang Gao[a]; Dejuan Kong[a]; Shurong Li[a]
[a] College of Chemistry and Environment Science, Hebei University, Baoding, People's Republic of China

Online publication date: 10 June 2010

To cite this Article Gao, Jungang , Kong, Dejuan and Li, Shurong(2008) 'Preparation of BPA Epoxy Resin/POSS Nanocomposites and Nonisothermal Co-curing Kinetics with MeTHPA', International Journal of Polymeric Materials, 57: 10, 940 — 956
To link to this Article: DOI: 10.1080/00914030802153397
URL: http://dx.doi.org/10.1080/00914030802153397

International Journal of Polymeric Materials, 57:940–956, 2008

ISSN: 0091-4037 print/1563-535X online
DOI: 10.1080/00914030802153397

Taylor & Francis
Taylor & Francis Group

Preparation of BPA Epoxy Resin/POSS Nanocomposites and Nonisothermal Co-curing Kinetics with MeTHPA

Jungang Gao, Dejuan Kong, and Shurong Li
College of Chemistry and Environment Science, Hebei University, Baoding, People's Republic of China

Polyhedral oligomeric silsesquioxanes epoxy resin (GM-POSS) was prepared from 3-glycidyloxypropyl-trimethoxysilane (GTMS) and methyl triethoxysilane (MTES) by hydrolytic condensation. GM-POSS was characterized using liquid chromatography/mass spectrometry (LC/MS). The epoxy value of GM-POSS is 0.23 mol/100 g. The LC/MS analysis indicates that T_8 and T_9 cages are the majority and contain some amount of T_{10}. The co-cured nanocomposites of BPA epoxy resin with GM-POSS using 3-methyl-tetrahydrophthalic anhydride (MeTHPA) as the curing agent were prepared and the co-curing kinetics was investigated by nonisothermal differential scanning calorimetry (DSC). The relationship between apparent activation energy E_a and the conversion α was obtained by the isoconversional method of Kissinger, and E_a is 68–78 kJ/mol. The results show that these curing reactions can be described by the Šesták-Berggren (S-B) equation, which includes two parameters, m and n. For different mass ratio of GM-POSS and BPAER, the two reaction orders, m and n, are in the range of 0.25∼0.42 and 0.52∼1.28, respectively. The curing kinetics can be described by the equations

$$\frac{d\alpha}{dt} = A\exp\left(-\frac{E_a}{RT}\right)\alpha^m(1-\alpha)^n$$

Keywords: curing kinetics, epoxy resin, phthalic anhydride, silsesquioxane

Received April 1, 2008; in final form April 14, 2008.

The authors gratefully acknowledge the financial support of the Nature Science Foundation (No. E2007000204) of Hebei Province, China.

Address correspondence to J. Gao, College of Chemistry and Environment Science, Hebei University, Baoding 071002, People's Republic of China. E-mail: gaojg@mail.hbu.edu.cn

INTRODUCTION

Epoxy resins have been used extensively, and the items prepared from epoxy resins as matrices of polymer composites are endowed with excellent adhesive strength, rigidity, mechanical properties, chemical alkali resistance, and so on. However, they are limited in many high-performance applications because of their brittleness and low thermal resistance. So, the heat resistance and toughness of cured products need to be improved. Factors that influence these properties of epoxy resins are the crosslink density and molecular chain structure. So, increased toughness and thermal resistance of epoxy resins is a research hotspot.

Organic-inorganic hybrid nanocomposite materials have attracted a great deal of attention because of their potential applications in optics, electronics, engineering and bioscience. Organic-inorganic hybrid polymers with an in situ-created inorganic phase are typical examples of nanocomposite materials, which have received significant interest in the past few years. The hydrolytic condensation of organotrialkoxysilanes, $RSi(OR')_3$, performed in the presence of water and an acid or base as catalyst, leads to products that are generically called polyhedral oligomeric silsesquioxanes (POSS). Species counted in POSS may vary from perfect polyhedra of formula $(RSi_iO_{1.5})_n$ ($n \geq 6$), denoted as T_n or as POSS, to partially condensed (but completely hydrolyzed) products of generic formula $T_n(OH)_m$, where $T = RSi_iO_{1.5\text{-}m/2n}$ [1–7]. These compounds have acquired increasing importance for the synthesis of functionalized organic-inorganic hybrid materials, because the polymers/silsesquioxanes nanocomposites combine the excellent properties of organic polymer materials with inorganic materials.

The POSS epoxy resins (POSSER) with an epoxy group connected to a silicon atom of the POSS have been synthesized, and the curing reaction with 4,4′-diaminodiphenylmethane (DDM) also has been studied [8–10]. We have synthesized the 3-glycidyloxypropyl-POSS (G-POSS) from hydrolytic condensation of 3-glycidyloxypropyl-trimethoxysilane (GTMS) with tetramethylammonium hydroxide as catalyst and investigated the curing behavior of G-POSS with 4,4′-diaminodiphenylsulfone (DDS) [11]. But the cured material of G-POSS with diamine is brittle because the density of epoxy groups is quite high on the G-POSS, which makes the curing material to form dense crosslink networks. In order to decrease the density of epoxy groups on the POSS, the 3-glycidyloxypropyl/methyl-POSS (GM-POSS) was prepared from co-hydrolytic condensation of 3-glycidyloxypropyl-trimethoxysilane and methyl triethoxysilane in a 1:1 mol ratio. The co-curing

nanocomposites of BPA epoxy resin with GM-POSS, using 3-methyl-tetrahydrophthalic anhydride (MeTHPA) as the curing agent, were prepared and the co-curing kinetics were investigated by nonisothermal differential scanning calorimetry (DSC) at different heating rates. The technologic parameters and kinetics equations of the curing reaction were obtained.

EXPERIMENTAL

Materials

3-glycidyloxypropyl-trimethoxysilane (GTMS) was supplied by Shenda Chem. Co., Beijing, China. Methyl triethoxysilane (MTES) was supplied by DeBang Chem. Co. of Yingcheng, Hubei, China; isopropyl alcohol (IPA), 3-methyl-tetrahydrophthalic anhydride (MeTHPA), tetramethylammonium hydroxide (TMAH), toluene, acetone and N,N-dimethyl-benzylamine (DMBA) were all analytically pure grade and were supplied by Beijing Reagent Co., China; bisphenol-A epoxy resin (BPAER) was supplied by Yueyang Chem. Co., China, the epoxy value is 0.51 mol/100 g; HPLC grade methanol was obtained from Tedia Co., of the USA.

Synthesis and Characterization of GM-POSS Epoxy Resin

The GM-POSS epoxy resin was synthesized by co-hydrolytic condensation of GTMS with MTES in a ratio of 1:1 mol (17.22 g GTMS and 12.98 g MTES). 7.8 g 5% TMAH aqueous solution and 100 mL IPA were placed into a four-necked flask equipped with stirrer, thermometer and condenser. After the reaction mixture was stirred for 6 h at 25°C, the water and IPA were removed in vacuum. Then the hydrolytic product was dissolved by adding 100 mL toluene and heated to 92°C, and the reaction maintained at this temperature for 4 h, during which the Si-O-Si bonds were formed through the reaction of intermolecular cyclization of Si-OH groups. After that, the toluene was removed in vacuum and the GM-POSS in form of viscous liquid was obtained, whose formula is $(RR'S_iO_{1.5})_n$, where R=CH_3, and R'=$CH_2CH_2CH_2OCH_2CH(O)CH_2$. The molecular structure is shown in Figure 1. The yield is above 90%, and the epoxy value is 0.23 mol/100 g determined by a literature procedure [12], which is consistent with theoretic value.

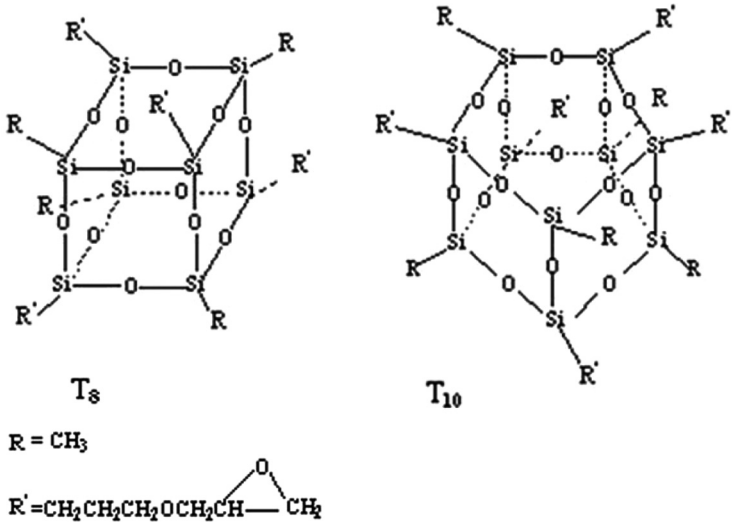

FIGURE 1 Cage structures of GM-POSS.

The LC/MS analysis was performed using an Agilent Zorbax SB-C18 (Agilent Co., USA).The mobile phase was 0.5% HAC water solution and 0.5% HAC methanol solution with volume ratio of 1:9. The flow rate was 0.25 mL/min and the injection volume was 1 μL. The column temperature was kept at 30°C.

The mass spectra were recorded with an ion trap mass spectrometer LCQ-DecaXP (Thermo Quest Co., USA) equipped with a UV spectrophotometer. The range of wavelengths detected was from 198 to 800 nm. The spectra were collected in the positive ion mode (MS^+), and a mass range of 400.00–1500.00 u(m/z) scanned with a 0.20–0.50 u(m/z) step size and a dwell time of 2.0 ms.

Preparation of DSC Samples and Characterization

Six samples were prepared according to mass per cent of GM-POSS in epoxy mixtures of GM-POSS with BPAER: 0% (No. 1), 10% (No. 2), 20% (No. 3), 30% (No. 4), 50% (No. 5), and 100% (No. 6). The GM-POSS and BPAER were mixed homogeneously at room temperature, then, MeTHPA in a stoichiometric ratio of one epoxy group to one carboxy group and 0.1% DMBA were added to the system. The curing reactions were carried out with differential scanning calorimeter (DSC, Diamond, Perkin Elmer Co., USA). The DSC instrument was calibrated with high-purity indium and operated under

20 mL/min nitrogen flow rate. Each sample (about 6 mg) was placed in a sealed aluminum sample pan. Dynamic scans were conducted from 40 to 200°C at selected heating rates of 5, 10, 15, and 20°C/min.

The distribution of silica was characterized by means of X-ray energy dispersive spectrometry (EDS). Resin was heated and pressed into 1.0 mm thickness plaque, and then was scanned by Vantage EDS (Thermo Noran Co., USA). The acceleration voltage was 25 kV and resolution was 128×128.

RESULTS AND DISCUSSIONS

LC/MS Analysis of GM-POSS

Recently, LC/MS analysis has become a very powerful tool for the investigation of siloxanes [12], and silsesquioxanes [13, 14]. In this study, LC/MS was used for the determination of the components of GM-POSS and the detailed structure. The molecular formula is $(RR'S_iO_{1.5})_n$, where R=CH_3, and  . But the GM-POSS is a mixture because the number of R and R' is variable in these POSS molecules. We can calculate the theoretic molecular mass: T_8 is varying between 537 g/mol and 1337.9 g/mol (from having no epoxy group to having 8 epoxy groups), with average value of 937.5 g/mol; T_9 is from 604.1 g/mol to 1505.2 g/mol and mean value of 1004.6 g/mol; T_{10} is in the range of 671.3 g/mol to 1672.4 g/mol and average value of 1171.8 g/mol. Figure 2 is the mass spectrum of the liquid chromatography determined by the experiment of LC/MS analysis. The mass data of some GM-POSS are shown in Table 1. As shown in Table 1, the GM-POSS is a mixture of T_8, T_{10}, and T_9. T_8 are the main products synthesized from GTMS and MTES by this method and some amount of T_{10} and T_9 also exist. The result is in agreement with the literature [10,11], but the ratio of T_{10}, T_8, and T_9 doesn't have any effect on the reaction with MeTHPA.

Curing Technologic Parameters and Apparent Activation Energy

The curing reactions for all six samples of GM-POSS/BPAER/MeTHPA were measured by the nonisothermal DSC method at heating rates of 5, 10, 15, or 20°C/min. The curing curves of the GM-POSS/BPAER/MeTHPA (No. 3) system arer shown in Figure 3. As can be seen from Figure 3, the heating rate shows great influence on the characteristic temperatures of the curing reaction. The initial

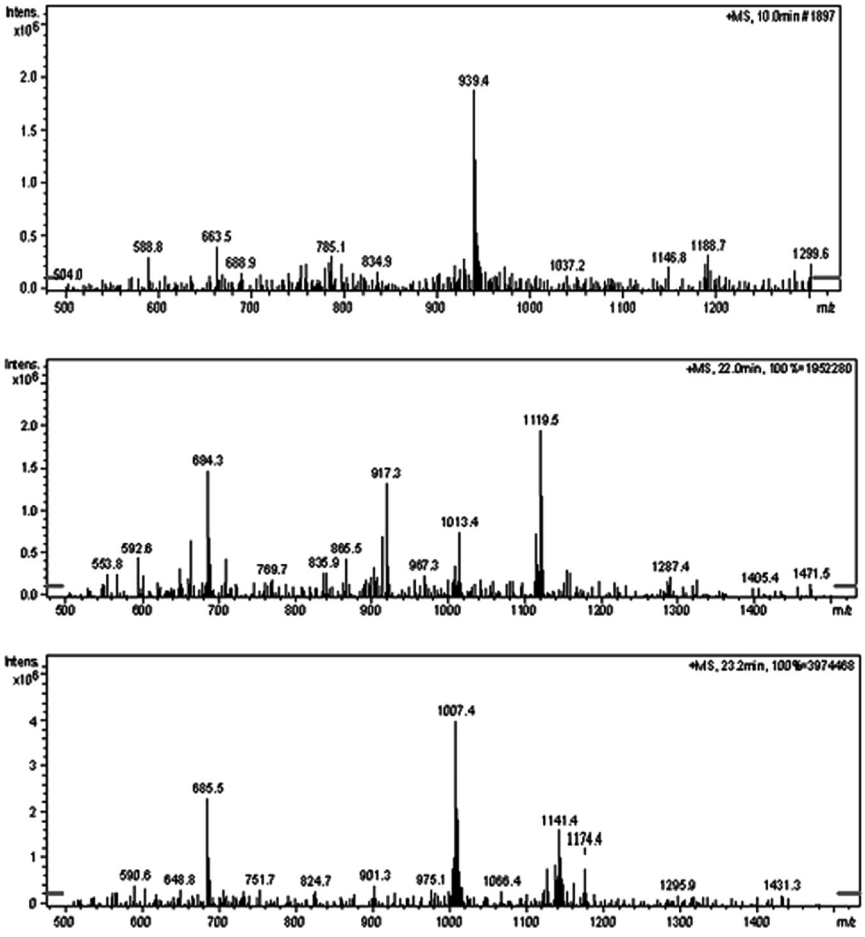

FIGURE 2 MS of the liquid chromatography.

TABLE 1 The Mass Data of GM-POSS

m/z(exp.)	Species
	T_8
939.4	$4R + 4R' + 2H^+$
1141.4	$2R + 6R' + 4H^+$
	T_9
1007.4	$5R + 4R' + 3H^+$
	T_{10}
1174.4	$5R + 5R' + 4H$

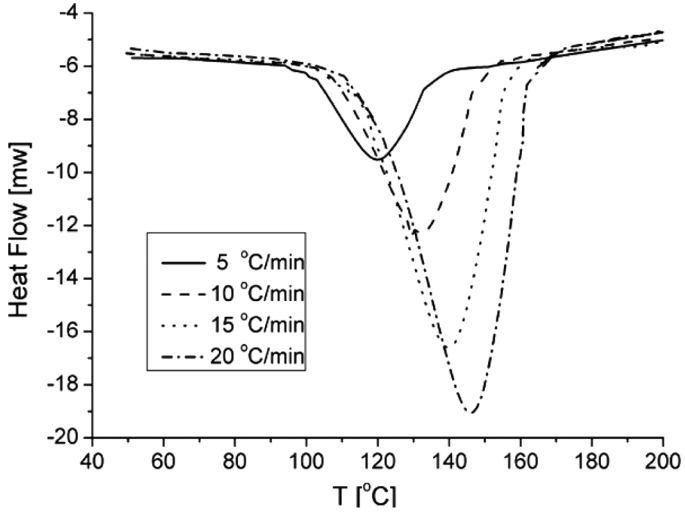

FIGURE 3 Dynamic DSC thermograms of of GM-POSS/BPAER/MeTHPA (No. 3) at different heating rates.

curing temperature (T_{icu}), the peak temperature (T_{pcu}) and the finishing temperature (T_{fcu}) increase with heating rate increases, and the temperature range of the curing reaction is broadened. The DSC curves of the GM-POSS/BPAER/MeTHPA system are all very smooth and have only single curing peak. This indicates that the compatibility of this system is very good and it can co-cure. Figure 4 is the distribution of GM-POSS in the cured products characterized by X-ray energy dispersive spectrometry (EDS). As can be seen from Figure 4, the distribution of GM-POSS in the cured product is homogeneous. Similar results were obtained from the other five samples under the same conditions, so that the organic-inorganic hybrid materials can be obtained by the method above.

From the plots of the initial temperature (T_{icu}), the peak temperature (T_{pcu}) and the finishing temperature (T_{fcu}) vs. heating rate β, we can obtain respectively the gel point of cured-system T_{gel}, curing peak temperature T_{pcu} and final temperature T_{fcu} at $\beta = 0$. As shown in Table 2, the curing temperature parameters have only a little difference for the six samples and indicate that the content of GM-POSS has little effect on the curing technologic parameters of the GM-POSS/BPAER/MeTHPA systems.

For the nonisothermal curing process, the Kissinger isoconversional method can be applied to different degrees of conversion, α [15,16].

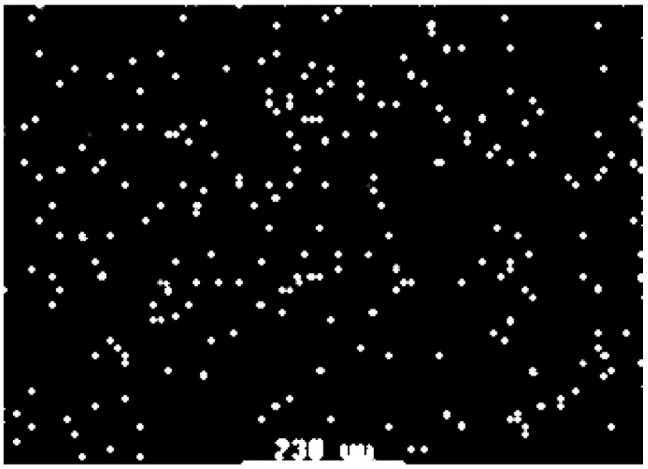

FIGURE 4 The distribution of GM-POSS in the cured product (No. 4).

Equation 1 is known as the Kissinger equation:

$$\ln\left(\frac{\beta}{T_p^2}\right) = \ln\left(\frac{AR}{E_a}\right) - \frac{E_a}{R}\cdot\frac{1}{T_p} \tag{1}$$

where A is the pre-exponential factor of the Arrhenius equation, T is the absolute temperature (K), R is the gas constant (8.314 J.mol/K), β represents the heating rate ($K\,\mathrm{min}^{-1}$), and E_a is the apparent activation energy. The relationships between α and the dynamic curing temperature T for the GM-POSS/BPAER/MeTHPA (No. 3) system are shown in Figure 5, and the relationships of $-\ln(\beta/T_\alpha^2)$ with $1/T_\alpha$ for No. 3 are shown in Figure 6. As seen from Figure 6, for a given conversion α, the apparent activation energy E_a can be obtained from the plot of $-\ln(\beta/T_\alpha^2)$ vs. $1/T_\alpha$. Thus, we can obtain E_a at different conversions α. The linear coefficients are all between 0.991 and 0.999, which shows that the curing systems well obey Kissinger's

TABLE 2 Data of T_{gel}, T_{pcu}, and T_{fcu} for Different Samples at $\beta = 0$

GM-POSS (%)	0%	10%	20%	30%	50%	100%
T_{gel}	92.16	94.43	94.26	94.43	92.74	93.36
T_{pcu}	120.25	116.53	112.96	111.73	108.45	112.37
T_{fcu}	141.51	142.87	140.69	140.22	134.24	136.13

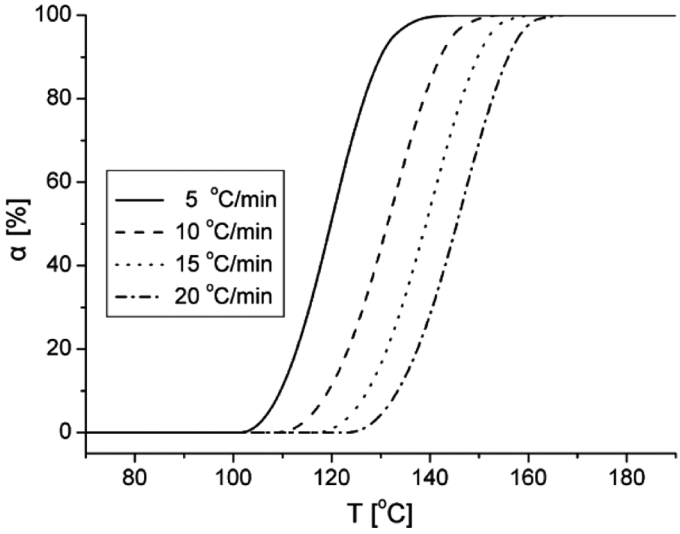

FIGURE 5 Relationship of conversion α vs. temperature T for sample 3.

kinetic model. By the same method, the relationships of E_α with α can be obtained for the other five samples. Figure 7 shows the variation of E_α with α for all samples in the interval of $0 \leq \alpha \leq 1$.

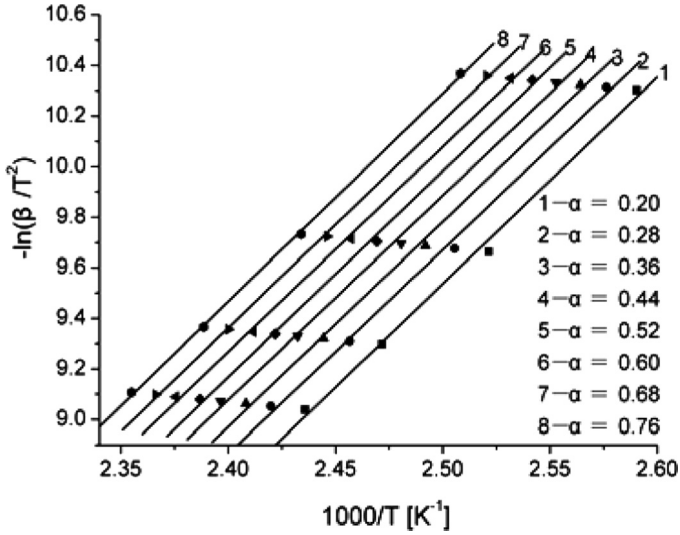

FIGURE 6 Relationship of $-\ln(\beta/T_\alpha^2)$ with $1/T_\alpha$ for sample 3 in the interval of $0.20 \leq \alpha \leq 0.76$.

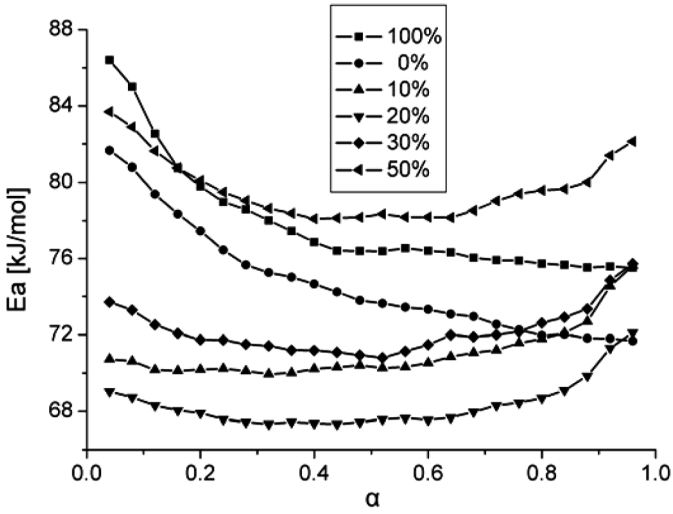

FIGURE 7 Relationship of E_a vs. α.

As seen from Figure 7, the E_a values change with α, and it shows that the mechanism of curing reaction for epoxy/MeTHPA is complex due to gelation and vitrification during the curing process. The values of E_a in the initial stage ($\alpha = 0$–0.15) are higher than those of any other time for all the samples. Then E_a tends to decrease slightly with the reaction progress, but has very little variation for conversion between 0.3 and 0.85 (except No. 1 and 6), which is the result of dynamic equilibrium in this stage. The higher E_a in the initial stage shows that the opening ring reaction of MeTHPA with oxygen anion or tertiary amine in DMBA is more difficult than the reaction of carboxyl anion with epoxy group, because MeTHPA is a stable five-member ring and has the p-π resonance nature, while the epoxy group is a unstable three-member ring. The E_a tends to decrease slightly with the reaction progress, which is associated with the hydroxyl group existing in the BPAER. Since the hydroxyl group can exist in a transition state (i.e., intermolecular hydrogen bonds) with epoxy group or MeTHPA, which could change the initial reaction mechanism, it may lead to a decreasing E_a [17]. On the other hand, the E_a increases slightly with the reaction progressing in the final stage for the bi-component system of GM-POSS/BPAER, which may be attributed to the higher crosslink density between two epoxy rings and MeTHPA, and the hindered mobility of the reactive groups. But for the No. 1 or No. 6 systems, the E_a does not increase in the last stage ($\alpha \geq 0.85$) and reduce with the reaction progressing and temperature raising under

the nonisothermal condition, which shows that the crosslink density of the one-component epoxy/MeTHPA system is not as high as the bi-component system of GM-POSS/BPAER. From Figure 7, we can also see that the higher the content of GM-POSS (except No. 3) the higher is E_a. The reason is that the GM-POSS in the curing process are highly constrained and encounter great energy barriers as the content of GM-POSS increases.

Nonisothermal Curing Kinetics Analysis

Generally, the kinetic equation of the nonisothermal curing system can be described as follows [15,18,19]:

$$\frac{d\alpha}{dt} \equiv \beta \frac{d\alpha}{dT} = K(T) f(\alpha) \tag{2}$$

where $\beta = dT/dt$ is a constant heating rate, $f(\alpha)$ is a dependent kinetic model function, K (T) is a temperature-dependent reaction rate constant and follows an Arrhenius form:

$$K(T) = A \exp\left(\frac{-E_a}{RT}\right) \tag{3}$$

The activation energy (E_a) can be determined by an isoconversional method if the value of $f(\alpha)$ is assumed to be the same at different heating rates when the value of α is the same. Then the values of E_a can be used to find the appropriate kinetic model which can best describe, $f(\alpha)$, the conversion function of the curing process [19,20]. The most suitable kinetic model can be evaluated with the functions of $y(\alpha)$ and $z(\alpha)$ according to Eqs. (4) and (5):

$$y(\alpha) = \left(\frac{d\alpha}{dt}\right) \exp(x) \tag{4}$$

$$(\alpha) = \pi(x) \left(\frac{d\alpha}{dt}\right) T/\beta \tag{5}$$

Where x is the reduced activation energy $(x = E_a/RT)$, and $\pi(x)$ is the expression of the temperature integral, which can be well-approximated using the fourth rational expression as in Eq. (6)

$$\pi(x) = \frac{x^3 + 18x^2 + 88x + 96}{x^4 + 20x^3 + 120x^2 + 240x + 120} \tag{6}$$

The $y(\alpha)$ function is proportional to the $f(\alpha)$ function, being characteristic for a given kinetic model. The shape and the maximum of both

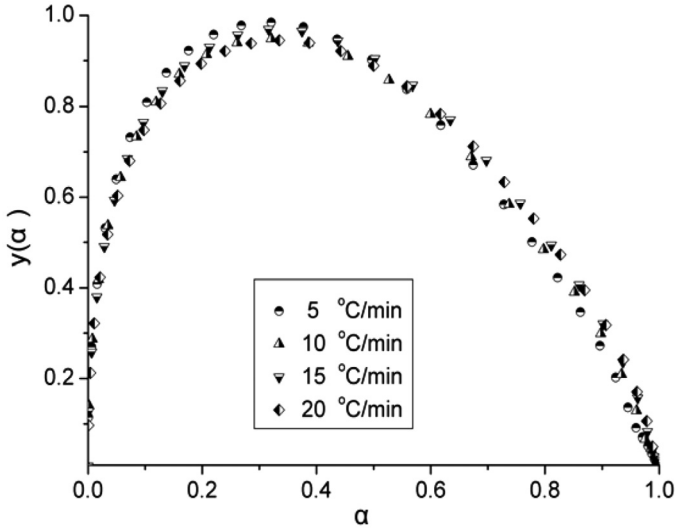

FIGURE 8 Variation of $y(\alpha)$ functions with conversion α.

$y(\alpha)$ and $z(\alpha)$ functions, α_M and α_p^{∞} normalized within the (0, 1) interval, give valuable information for determination of the most suitable kinetic model [19–21].

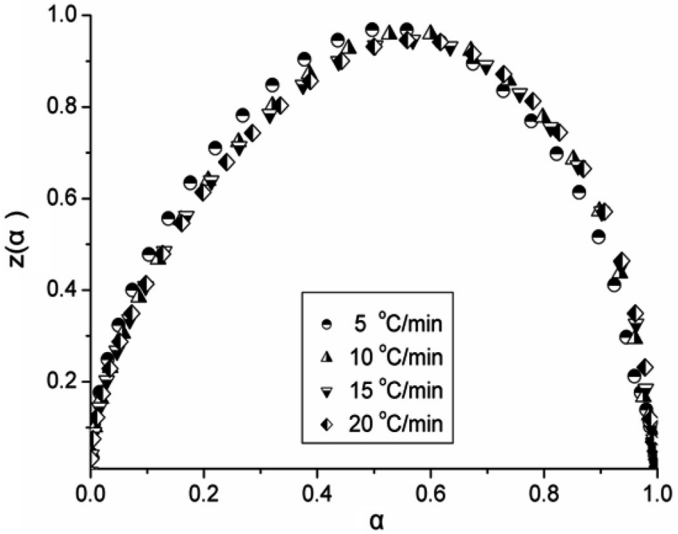

FIGURE 9 Variation of $z(\alpha)$ functions with conversion α for for No. 3.

Using the value of E_a and knowing the kinetic model, the pre-exponential factor A can be calculated according to Eq. (7)

$$A = -\frac{\beta x_p}{Tf'(\alpha_p)}\exp(x_p) \tag{7}$$

Where $f'(\alpha_p)$ is the differential form of the kinetic model $[df(\alpha)/d\alpha]$, and α_p is the conversion corresponding to the maximum on the DSC curve.

So, in our present research, the average value of E_a was used to calculate both $y(\alpha)$ and $z(\alpha)$ functions with Eqs. (4) and (5), respectively. Figures 8 and 9 show the normalized $y(\alpha)$ and $z(\alpha)$ functions of sample No. 3 at different heating rates.

From Figures 8 and 9, the values of α_M and α_p^∞ (the value of α while $y(\alpha)$ or $z(\alpha)$ gets the maximum value, respectively) of No. 3 can respectively be obtained. With the same method, the values of α_M and α_p^∞ for other samples, together with α_P (the α maximum at the DSC peak), can be obtained are shown in Table 3.

TABLE 3 α_p, α_M, and α_p^∞ Values Evaluated with the DSC Data of Six Samples

Sample	Heating rate (°C/min)	α_p	α_M	α_p^∞
No. 1	5	0.665	0.319	0.676
	10	0.676	0.333	0.689
	15	0.665	0.302	0.684
	20	0.664	0.329	0.689
No. 2	5	0.562	0.310	0.578
	10	0.595	0.320	0.609
	15	0.589	0.329	0.610
	20	0.591	0.336	0.605
No. 3	5	0.509	0.317	0.525
	10	0.549	0.314	0.563
	15	0.546	0.335	0.569
	20	0.559	0.335	0.573
No. 4	5	0.471	0.271	0.490
	10	0.507	0.289	0.522
	15	0.515	0.304	0.536
	20	0.525	0.310	0.539
No. 5	5	0.413	0.229	0.431
	10	0.457	0.235	0.469
	15	0.471	0.253	0.491
	20	0.479	0.246	0.493
No. 6	5	0.455	0.200	0.499
	10	0.502	0.213	0.530
	15	0.512	0.217	0.537
	20	0.519	0.221	0.541

TABLE 4 Kinetic Parameters Evaluated for Six Samples

Sample GM-POSS (%)	Heating rate (°C/Min)	*Ea* (kJ/mol)	p	lnA	Mean	n	Mean	m	Mean
No. 1	5	74.739	0.469	27.841	28.647	0.475	0.523	0.223	0.248
	10		0.499	28.608		0.543		0.271	
	15		0.434	28.879		0.504		0.218	
	20		0.489	29.261		0.572		0.279	
No. 2	5	71.100	0.450	27.125	27.895	0.752	0.702	0.338	0.336
	10		0.471	27.756		0.673		0.317	
	15		0.492	28.202		0.694		0.341	
	20		0.506	28.497		0.689		0.349	
No. 3	5	68.373	0.465	26.692	27.371	0.948	0.829	0.441	0.399
	10		0.459	27.198		0.788		0.361	
	15		0.505	27.696		0.822		0.415	
	20		0.504	27.897		0.758		0.382	
No. 4	5	72.257	0.372	27.945	28.692	1.099	1.010	0.409	0.419
	10		0.407	28.586		1.000		0.407	
	15		0.436	28.987		0.978		0.427	
	20		0.450	29.249		0.962		0.433	
No. 5	5	79.678	0.298	30.540	31.219	1.433	1.288	0.428	0.408
	10		0.308	31.128		1.282		0.395	
	15		0.338	31.474		1.255		0.424	
	20		0.327	31.735		1.181		0.386	
No. 6	5	77.891	0.251	29.422	30.136	1.207	1.121	0.302	0.302
	10		0.271	30.053		1.121		0.303	
	15		0.277	30.399		1.088		0.301	
	20		0.283	30.668		1.068		0.302	

As can be seen from Table 3, the values of α_M are lower than those of α_P, whereas the values of α_p^∞ are lower than 0.632 except No. 1. In accordance with the results of Málek on the kinetics of the curing reaction of epoxy resins under nonisothermal conditions [20], the studied curing systems can be described with the two-parameter autocatalytic kinetic model (i.e., the Šesták-Berggren equation) [22]:

$$f(\alpha) = \alpha^m(1-\alpha)^n \tag{8}$$

Where m and n are curing reaction orders.

From Eqs. (2), (3), and (8), we can obtain Eq. (9) as follows:

$$\ln\left[\left(\frac{d\alpha}{dt}\right)e^x\right] = \ln A + n\ln[\alpha^p(1-\alpha)] \tag{9}$$

where $x = E_a/RT$, $p = \alpha_M/1-\alpha_M$.

The kinetic exponent n can be obtained from the slope of $ln[(d\alpha/dte^x]$ vs. $ln[\alpha^p(1-\alpha)]$ and $m = pn$. Table 4 lists some kinetic

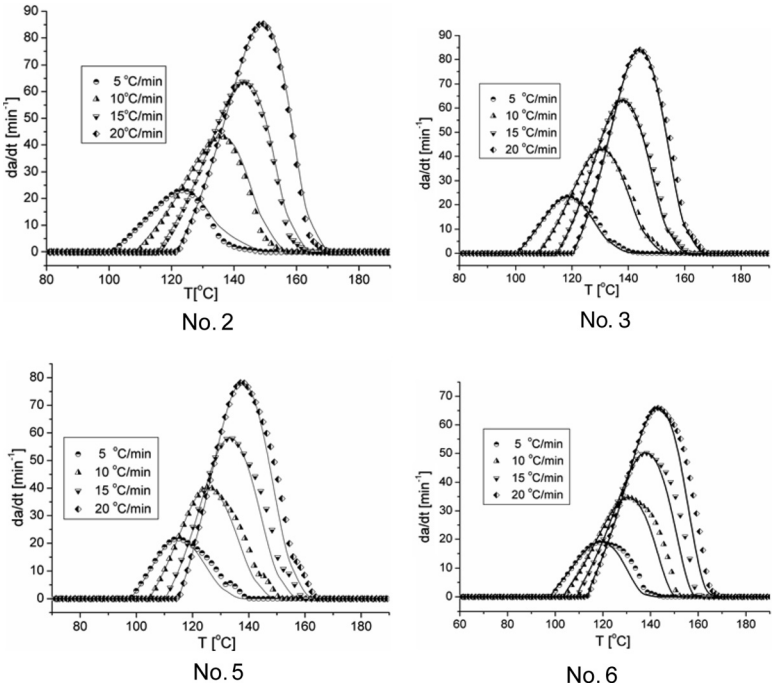

FIGURE 10 Comparison of experimental (dots) data and calculated (full lines) values: plots of reaction rate $d\alpha/dt$ vs. T for four samples of No. 2, 3, 5, and 6.

parameters evaluated from the proposed Šesták-Berggren (S-B) kinetic model. As is shown in Table 4, the variation of the kinetic parameters with the heating rates is within the experimental error limit (within 10% of the average value).

In order to verify the correctness of the kinetic model proposed with the *S-B* equation, we calculated the values of $d\alpha/dt$ using the data listed in Table 3 and simulated the curves of $d\alpha/dt$ vs. T. Figure 10 presents the comparison of experimental and theoretical values for four out of the six samples. As can be seen from Figure 10, the theoretical curves all match well the experimental points. In other words, the two-parameter *S-B* model can be well-used for all the studied curing systems, and these systems follow the kinetic equation

$$\frac{d\alpha}{dt} = A \exp\left(-\frac{E_a}{RT}\right) \alpha^m (1-\alpha)^n$$

Where n is between 0.52 and 1.28, and m is between 0.25 and 0.42.

CONCLUSIONS

1. The polyhedral oligomeric silsesquioxanes epoxy resin (GM-POSS) which has a lower density of epoxy group can be prepared by co-hydrolytic condensation of 3-glycidyloxypropyl-trimethoxysilane and methyl triethoxysilane, and T_8 are the main products but contain some amounts of T_{10} and T_9.
2. The GM-POSS with bisphenol-A epoxy resin has quite good compatibility and can co-cure with 3-methyl-tetrahydrophthalic anhydride. The apparent activation energy, E_a, of the curing reaction was obtained by the isoconversional method of Kissinger, and is 68–78 kJ/mol.
3. These curing reactions can be described with the Šesták-Berggren (S-B) model, which includes two parameters of m and n, and the kinetic equations can be expressed as: $d\alpha/dt = A\exp(-E_a/RT)\alpha^m(1-a)^n$.

REFERENCES

[1] Mori, H., Lanzendorfer, M. G., and Muller, A. H. E., *Macromolecules* **37**, 5228 (2004).
[2] Choi, J., Yee, A. F., and Laine, R. M., *Macromolecules* **36**, 5666 (2003).
[3] Ignacio, E., Dell' Erba, D. P., Fasce, R., and Williams, J. J., *J. Organ. Metal. Chem.* **686**, 42 (2003).
[4] Baney, R. H., Itoh, M., Sakakibara, A., and Suzuki, T., *Chem. Rev.* **95**, 1409 (1995).
[5] Hu, C. Y., Tan, Y., and Yuan, C. Y., *Chin. Sci. Bul.* **17**, 1817 (1999).
[6] Liu, C. J., Chang, Z. J., and Li, X. D., *Chinese Polymer Materials Science and Engineering* **21**, 84 (2005).
[7] Lu, T. L., Liang, G. Z., Gong, Z. H., Ren, P. G., Zhang, Z. P., *Chin. Polym. Bull.* **1**, 15 (2004).
[8] Chen, W. Y., Wang, Y. Z., and Kuo, S. W., *Polymer* **45**, 6897 (2004).
[9] Choi, J., Kim, S. G., and Laine, R. M., *Macromolecules* **37**, 99 (2004).
[10] Saito, H., Isosaki, M., and Ando, H., *JP, Kokai* 285387(2002).
[11] Gao, J., Jiang, C., and Zhang, X., *Intern. J. Polym. Mater.* **56**, 65 (2007).
[12] Braun, D., Cherdron, H., and Kern, W., Ed., Huang, B. (1981). *Techniques of Polymer Syntheses and Characterization*, China Sci. Publishing. Co., Beijing, pp. 294 (in transition).
[13] Jaumann, M., Rebrov, E. A., Kazakova, V. V., Muzafarov, A. M., Goedel, W. A., and Moller, M., *Macromol. Chem. Phys.* **204**, 1014 (2003).
[14] Gidden, J., Kemper, P. R., Shammel, E., Fee, D. P., Anderson, S., and Bowers, M. T., *J. Intern. J. Mass Spectr.* **222**, 63 (2003).
[15] Jubsilp, C., Damrongsakkul, S., Takeichi, T., and Rimdusit, S., *Thermochimica Acta* **447**, 131 (2006).

[16] Ozawa, T., *J. Thermal Analysis* **2**, 301 (1979).
[17] Ehlers, J. E., Rondan, N. G., Huynh, L. K., Pham, H., Marks, M., and Truong, T. N., *Macromolecules* **40**, 4370 (2007).
[18] Xu, G., Shi, W., and Shen, S., *J. Polym. Sci.: Part B: Polym. Phys.* **42**, 2649 (2004).
[19] Rosu, D., Cascaval, C. N., Mustata, F., and Ciobanu, C., *Thermochimica Acta* **383**, 119 (2002).
[20] Málek, J., *Thermochim Acta* **200**, 257 (1992).
[21] Rosu, D., Mititelu, A., and Cascaval, C. N., *Polym. Test* **23**, 209 (2004).
[22] Šesták, J. and Berggren, G., *Thermochim Acta* **3**, 1 (1971).